



Compound flood potential from storm surge and heavy precipitation in coastal China

Jiayi Fang¹, Thomas Wahl², Jian Fang³, Xun Sun¹, Feng Kong⁴, Min Liu¹

¹Key Laboratory of Geographic Information Science (Ministry of Education), School of Geographic Sciences, East China Normal University, Shanghai, 200241, China

²Department of Civil, Environmental, and Construction Engineering and National Center for Integrated Coastal Research, University of Central Florida, 12800 Pegasus Drive, 32814 Orlando, USA

³College of Urban and Environmental Science, Central China Normal University, Wuhan, China

⁴School of Public Policy and Management, Tsinghua University, Beijing 100084, China

10 *Correspondence to:* Jiayi Fang (jyfang@geo.ecnu.edu.cn)

Abstract. The interaction between storm surge and concurrent precipitation can cause greater flooding impacts than either in isolation. This paper investigates the potential compound effects from these two flooding drivers along the coast of China. Statistically significant dependence between them exists at the majority of locations that are analysed, but the strength of the correlation varies spatially and depending on how extreme events are defined. In general, we find higher dependence at the south-eastern tide gauges (TGs) (latitude < 30°N) compared to the northern TGs. Seasonal variations in the dependence are also evident. Overall there are more sites with significant dependence in the typhoon season, especially in the summer. Accounting for past sea level rise further increases the dependence between flooding drivers and future sea level rise will hence likely lead to an increase in the frequency of compound events. We also find notable differences in the meteorological patterns driving compound and non-compound events. Compound events at south-eastern TG sites are caused by low-pressure systems with similar characteristics across locations, including high precipitable water content (PWC) and strong winds that generate high storm surge. Based on historical disaster damages records of Hong Kong, compound flood events account for the vast majority of damages and casualties, compared to univariate flooding events, where only one flooding driver occurred. Given the large coastal population and low capacity of drainage systems in many Chinese urban areas, these findings highlight the necessity to incorporate compound flooding and its potential changes in a warming climate into risk assessments, urban planning, and the design of coastal infrastructure and flood defences.

Keywords. Compound flood, Storm surge, Precipitation, China



30 1 Introduction

Floods are among the costliest and deadliest disasters globally (Hu et al., 2018). In recent years, a series of devastating compound flooding events occurred, such as Hurricane Isaac in 2012, Typhoon Haiyan in 2013, Hurricanes Irma and Florence in 2018, and Typhoon Lekima in 2019. Despite improvements in flood defences, flood forecasting, and warnings, these flood events caused devastating impacts, in parts
35 due to the limited understanding of compound floods in coastal regions. Flooding along the coast can arise from three main sources: 1) extreme sea levels (comprised of storm surge, high astronomical tides, and/or waves (coastal flood)); 2) river discharge (fluvial flood); and 3) direct surface run-off from rainfall (pluvial flood) (Hendry et al., 2019). Floods in coastal areas are frequently caused by more than one driver,
40 often much greater than from either flood driver occurring in isolation (Leonard et al., 2014; Zscheischler et al., 2018; Hao et al., 2018). Exploring the probabilities of compound flood events and understanding their driving processes is important for flood mitigation and risk reduction in a warming climate (Wahl et al., 2015).

A growing number of studies investigated compound flooding in recent years. At the global scale,
45 dependence between storm surge and river discharge has been investigated based on observational data (Ward et al. 2018) and model hindcasts (Bevacqua et al., 2020; Couasnon et al., 2020). The relationship between storm surge and wind waves was assessed by Marcos et al. (2019). At the regional scale, compound flood assessments have been undertaken for Australia (Zheng et al., 2014; Wu et al., 2018), the
50 USA (Wahl et al., 2015), the UK (Svensson and Jones, 2002, 2004; Hendry et al., 2019), and Europe (Petroliagkis et al., 2016; Paprotny et al., 2018; Bevacqua et al., 2019; Ganguli and Merz, 2019). Other studies focused on specific locations, such as the Netherlands (van den Hurk et al., 2015); Fuzhou, China (Lian et al., 2013); Taiwan, China (Chen and Liu, 2014), or the North Sea (Khanal et al., 2019). Most of these studies investigated the dependence between two hazards, such as storm surge and river discharge, storm surge and waves, or storm surge and rainfall.

55 For China, a comprehensive regional assessment of compound flooding is currently missing. Low-lying coastal areas (elevation less than 10 m) in China only account for 2% of the national land, but account for



more than 12% of the national population (Liu et al., 2015; Fang et al., 2020). At the same time, these areas are experiencing frequent coastal disasters from tropical cyclones (TCs) and storm surges, among others. Coastal flooding has caused more than US\$ 71 billion direct economic losses and 4,376 fatalities
60 from 1989 to 2014 (Fang et al., 2017). Flood risk is likely increasing in China due to climate change (most notably sea level rise), as well as human factors (e.g. human-induced subsidence) (Fang et al., 2020; Jiang et al., 2020; Wu et al., 2005; Wu et al., 2017). Meanwhile, fast urbanisation in China has led to more people and economic assets exposed to hazards (Fang et al., 2018; Du et al., 2018), and has also prompted irrational urban planning, increased areas of urban impervious surface, and low capacity drainage systems
65 (Cheng, 2020). For example, the capacity of the local drainage system of Shenzhen City is designed to drain the surface runoff associated with a 2-year return period (Urban Planning & Design Institute of Shenzhen, China, 2008). As drainage facilities are often under-designed and/or have not been upgraded, surface runoff during storms frequently exceeds the drainage capacity resulting in flooding damages in low-lying areas (Qin et al., 2013). Despite the relevance of compound flood risk for coastal China, the
70 associated probabilities and driving mechanisms have not been explored at broad spatial scales at the national level.

A limited number of studies have assessed different aspects of compound flooding for China. Lian et al. (2013) and Xu et al. (2014) investigated the joint probability, using copulas, of extreme precipitation and storm tide and associated changes for Fuzhou city. Both studies showed that the joint impacts from surge
75 and precipitation were much higher than from each individually; this is currently ignored in the design of flood defences. Xing et al. (2015) analysed joint return periods of precipitation and runoff in the upper Huai River Basin in China. Ye et al. (2018) estimated compound hazard severity of TCs considering extreme wind and precipitation. Changes in storm surges and precipitation in China have also been investigated separately, showing significant increases in extreme precipitation in parts of the southwest
80 and south China coastal areas (Zhai et al., 2005). Similarly, significant increases in sea level extremes have been reported (Feng et al., 2014; Feng et al., 2019), and attributed to both changes in mean sea level (MSL) and in the wind driven storm surge component (Feng et al., 2015). However, these previous studies were mostly local, they neglected seasonal characteristics, and weather circulation patterns driving compound events were not assessed. In this study, we use the most comprehensive records of storm surge



85 and precipitation to investigate dependencies and incidences of compound flooding associated with storm surge and heavy precipitation along the coast of China, as well as the large scale weather systems causing compound events.

In this context our three main objectives are to: 1) identify and collate compound events from storm surge and precipitation, and analyse their dependence, including the role of sea level rise and seasonality; 2) understand the driving weather patterns of compound/non-compound events; and 3) compare damages
90 caused by compound and non-compound events.

2 Data

Most tide gauge (TG) data are kept confidential in China; thus, we obtained hourly sea-level data of 11 TGs with at least 20-year lengths along the Chinese coast from the University of Hawaii Sea Level Center
95 (Caldwell et al., 2015). Locations of TGs and the time series' lengths are shown in Fig. 1. The stations are located south of the Shandong peninsula in China, where tropical cyclone impacts are most severe. Nine of the 11 TG stations have about 20 years of data (1975-1997), Xiamen and Hong Kong have 46 years (1954-1997) and 52 years (1962-2014), respectively.

[Fig. 1]

100 Storm surge is extracted using the MATLAB `t_tide` package (Pawlowicz et al., 2002) by applying a year-by-year harmonic tidal analysis with 67 constituents. It also effectively removes the MSL influence. The data has been checked for common errors and 75% completeness of each year is required. An offset in the Hong Kong data is adjusted by shifting the earlier data by 1.02 cm, following Ding et al. (2002).

Cumulative daily precipitation records from 1951-2015 are collected from China Meteorological
105 Administration. The closest meteorological station is chosen to match each TG station, and 9 out of 11 TGs are less than 25 km distance. The time series of precipitation observations are usually longer and more complete than TG observations; thus TG data availability determines the lengths of overlapping periods available for the analysis presented here.



To identify weather patterns typically associated with compound and non-compound events, sea surface
110 pressure (SLP), precipitable water content (PWC), and wind fields are used from the Twentieth Century
Reanalysis Project Version 2c (Compo et al., 2011).

To compare impacts caused by compound and non-compound events, we employ a typhoon database
developed by Yap et al. (2015), which includes historical typhoon records from 1951 to 2012, with the
main focus on Hong Kong, Taiwan, and the south-eastern Chinese coastal provinces of Zhejiang, Fujian,
115 Guangdong and Hainan. The database contains information of 853 typhoons in total, with records of direct
normalized economic loss (in US\$), death toll, and number of people affected.

3 Methodology

3.1 Selecting compound events

The combination of storm surge and precipitation can exacerbate the flood impacts in different ways
120 (Wahl et al., 2015). First, both heavy precipitation and extreme sea levels (storm surge with high tides)
can coincide, leading to more severe floods. This often happens during typhoon events. Second, impacts
of a storm surge already causing flooding will increase when significant precipitation occurs at the same
time, although the precipitation itself may not be considered extreme. Third, a moderate storm surge can
block freshwater water drainage and high precipitation occurring at the same time can lead to more serious
125 flooding (as compared to the same rain event coinciding with low sea level). To capture all of those
mechanisms, we investigate the relationship of storm surge and precipitation for two distinct cases: in
Case 1 we select extreme storm surge events and the corresponding precipitation within ± 1 day of the
surge; in Case 2 we select extreme precipitation events and the corresponding storm surges within ± 1
day of the precipitation (Fig. 2).

130 *[Fig. 2]*

We use the peaks over thresholds (POT) method to select extreme events. The POT method refers to
selecting events over a high threshold within a certain time span. The annual maximum approach is widely
used for sampling extreme events. However, it would be not appropriate here as time series of 9 out of 11



TGs in China only have around 23 years of data, which would lead to small sample sizes. Furthermore,
135 the second or third largest values in a given year may be larger than the annual maximum in another year
(Coles et al., 2001; Arns et al., 2013). To test the sensitivity of the results to the threshold selection, we
employ thresholds related to eight percentiles ranging from 95% to 99.5%, i.e., 95%, 96%, 97%, 98%,
98.5%, 99%, 99.25% and 99.5%. Independence of the POT sample was achieved using a declustering
time of 3 days. We also test how the inclusion of sea level rise affect the compound events (in Section
140 4.2).

3.2 Dependence analysis

Kendall's rank correlation coefficient τ is employed to measure dependence between storm surge and
precipitation. In Case 1, storm surges sometimes could occur without any precipitation, and this leads to
ties (i.e., several zero values) affecting the dependence analysis. We use the same method as suggested in
145 Kojadinovic (2010) and Wahl et al. (2015) by assigning ranks randomly, repeating the procedure 100
times and calculating the average rank correlation. To better understand the influence of seasonality,
dependence is assessed for the full year as well as for summer (June to August), autumn (September to
November), and the typhoon season (July to October) separately.

We also assess how compound event frequencies are affected by MSL rise along coastal China. The
150 effects of MSL are initially removed during the harmonic tidal analysis. In order to assess the compound
effects under nonstationary conditions, we repeat the analysis but keep the MSL influence and extract
surge events by only removing the tidal influence, i.e., total water level minus tide. Then we re-count the
numbers of compound events (i.e. falling in Zone 1 in Fig. 2) with MSL included.

3.3 Weather patterns

155 To investigate the meteorological patterns that drive compound and non-compound flood events, sets of
the two types of events are selected based on a threshold of 98%. Compound events refer to joint
occurrences of high storm surge and heavy precipitation (Zone 1 in Fig. 2). Non-compound events refer
to only high storm surge (Zone 2 in Fig. 2) or only heavy precipitation (Zone 3 in Fig. 2). SLP, PWC, and
wind fields on the days are selected to match days when compound/non-compound events occurred, then



160 they are averaged into composites to represent reference synoptic-scale weather patterns favouring compound events.

3.4 Losses associated with compound and non-compound events

In order to quantify the differences in impacts caused by compound and non-compound events, we employ historical damage records. We take Hong Kong (TG 7) as an example; it also has the most historical
165 damage data available, from 1962 to 2012. The other ten TGs cannot directly be linked to the damage database, as the typhoon database from Yap et al. (2015) only collected damage records at province level. Therefore, to compare damages caused by compound and non-compound events, we match the days when the selected compound/non-compound events (separated in the same way as for the synoptic weather type analysis) occurred with records in the database including information of death toll, people affected, and
170 economic losses.

4 Results

4.1 Dependence between storm surge and precipitation

Figure 3 demonstrates dependence between storm surge and precipitation in Case 1 and Case 2, also indicating the impact of the thresholds (95% to 99.5%) which can influence the correlation. For Case 1,
175 south coastal China, which is more affected by TCs (Fig. 1), exhibits higher dependence than the northern part. Overall, Case 1 dependence is also higher than Case 2 dependence and we identify more locations with significant dependence, 11 TGs in Case 1 and 7 TGs in Case 2, respectively.

[Fig. 3]

Haikou (TG10) shows the highest positive dependence for both cases among all TGs. Kanmen (TG4)
180 shows the second highest positive dependence for Case 1, and also shows relatively high dependence in Case 2. Lianyungang (TG2) and Beihai (TG9) show insignificant dependence for both cases, indicating that a limited number of compound events occurred at those sites (Fig. 3c and 3d). Shanwei (TG6) and Zhapo (TG8) show high positive dependence in Case 1, but insignificant dependence in Case 2, meaning



185 that high storm surge is often accompanied by high rainfall but not the other way round. The opposite is true for Lusi (TG3) which has positive dependence in Case 2, but insignificant dependence in Case 1.

At most locations the dependence increases when higher thresholds are used to sample extremes (Fig. 3c and 3d). There are exceptions however, for example, Haikou (TG10) in Case 2 shows higher dependence with a threshold of 99% than 99.5%. At some TGs dependence becomes insignificant due to small sample sizes when thresholds are very high, indicating the trade-off between bias and variance in the threshold selection.

190

4.2 Effects of sea level rise on compound event frequencies

8 out of 11 TGs show an increase of compound events when MSL influence is included (Fig. 4), number of compound events of TG 10 (Haikou) remain unchanged. For example, at Lianyungang (TG2) and Beihai (TG9), only one compound event is identified when MSL is removed, while this number increases to 22 and 26, respectively, with MSL included. It indicates that coastal China will experience an increasing frequency of compound flood events with future MSL rise. This is in line with Moftakhari et al. (2017) and Bevacqua et al. (2019), who also report that SLR will lead to more compound events. SLR not only increases the probability of coastal flooding from storm surges (Buchanan et al., 2017), but also poses an additional threat for coastal communities susceptible to compound events. Meanwhile, other flood drivers, such as precipitation, river discharge, waves, and TCs, can also exhibit nonstationarity leading to increased (compound) flood risk (Kundzewicz et al., 2019). Observations from the last five decades and numerical model studies (Lai et al., 2020) indicate a slowdown of TCs, which would likely favour more extreme rainfall during the events as compared to fast-moving TCs.

195

200

[Fig. 4]

205 4.3 Seasonal variation

To better understand the timing of events leading to joint dependence throughout the year (as identified in Section 4.1), the influence of seasons is investigated. TCs are active over the western North Pacific during July to October (He et al., 2015). Thus, four periods are considered: typhoon season (July-October),



summer (July-August), autumn (September-November), and whole year. The seasonal dependences for
210 different thresholds in the POT sampling are displayed in Fig. 5. Lianyungang (TG2), Lusi (TG3), and
Beihai (TG9) show insignificant dependence for both cases and all seasons and thresholds and are
therefore not included.

[Fig. 5]

For Case 1, multiple TGs show stronger dependence in summer and in the typhoon season compared to
215 the whole year, such as Kanmen (TG4), Shanwei (TG6), and Hong Kong (TG7). Compared to Case 1,
there are fewer locations with significant dependence for Case 2. Shanwei (TG6) and Zhapo (TG8) show
insignificant dependence in Case 2, while significant positive dependence is found in Case 1. For most
TGs, dependence varies with the increase of thresholds. However, for multiple TGs, such as Kanmen
(TG4), Shanwei (TG6), Zhapo (TG8), Haikou (TG10), and Dongfang (TG 11) dependence continuously
220 increases with higher thresholds. Again, for some TGs, dependence becomes insignificant for high
thresholds, e.g. Hong Kong (TG7), indicating the importance of threshold selection, especially when
records are short.

TGs from Kanmen (TG4) to Dongfang (TG11) are most affected by TCs, and show high dependence for
Case1, especially in summer and in the typhoon season. Xiamen (TG5), is an exception, likely because
225 Taiwan Island weakens the intensity of cyclones before reaching Xiamen. Stronger dependence in autumn
is found for southern TGs (latitude $< 25^{\circ}\text{N}$), such as Hong Kong (TG7), Beihai (TG9), and Dongfang
(TG11), where typhoons still occur autumn. The dependences in typhoon season are similar with the
whole year, which indicates that most compound events occur in the typhoon season. For example, 80%
compound events (Zone 3 in Fig. 2) for Hong Kong (TG7) and 97.5% for Haikou (TG10) occurred in the
230 typhoon season. South-east coastal China is not only affected by TCs, but also by summer monsoon
precipitation from the Northwest Pacific Subtropical High. The summer monsoon brings continuous
precipitation since June to August in southern China. Thus, the dependence is higher in the summer
compared to the typhoon season. It has been reported that an abrupt increase of intense typhoons occurred
in September after the mid-2000s for south China (He et al., 2016), which could affect the seasonality of



235 compound events. However, from the results shown in this study, this pattern is not captured due to limited observation (most observations end in 1997).

4.4 Links to weather patterns

We derived composite plots of synoptic conditions of SLP, PWC, and wind fields that drive compound (both high storm surge and heavy precipitation) and non-compound events (high storm surge or heavy
240 precipitation only) across coastal China. To illustrate the results, we focus on Kanmen (TG4) and Shanwei (TG6) on the east and south coast of China, which both have been frequently affected by typhoons (Fig. 6 and Fig. 7). Results for the other nine stations are shown in Supplementary Figs. S1- S9. Based on the thresholds we selected to identify compound and non-compound events (see Method 3.3), we identify 15 compound events for Kanmen (TG4) and 21 events for Shanwei (TG6), respectively.

245 *[Fig. 6]*

The meteorological patterns in SLP, PWC, and wind fields are distinctly different across the three event types. At Kanmen (TG4), compound events are associated with a well-defined low-pressure system with strong east-west and south-westerly winds transporting moist air toward the south-eastern coast of China (Fig. 6a-c). Non-compound events with only high storm surge exhibit a distinct pressure gradient along
250 the coast (Fig. 6d). As expected, the wind speed is much stronger along the coast for this case (Fig. 6e) compared to the one where only precipitation is high (Fig. 6h), and the northern high wind drives moist air away from the site of interest. The differences in PWC patterns for compound and non-compound events are more pronounced (Fig. 6c, f, i). There is low PWC for the type of only high storm surge events (Fig. 6f), while high PWC from the Bay of Bengal and cross-equatorial flow is observed for the other two
255 types of events.

[Fig. 7]

At Shanwei (TG 6), similarly to Kanmen, the meteorological patterns in SLP show a cyclone-structure for both compound events and non-compound events with only high storm surge (Fig. 7a and 7d). For events with high storm surge only, there is a distinct pressure gradient and strong wind speed (Fig. 7e).
260 The PWC is low for the high storm surge events and high for compound and precipitation only events



(Fig. 7c, f, i). For precipitation only events, flows from the Bay of Bengal and cross-equatorial flow is observed, and south-eastern wind drives moist air to the site of interest for compound events and high precipitation only events (Fig. 7b and 6h).

The results for other stations are similar (Supplementary Figs. S1-S9). For compound events, synoptic
265 weather patterns for south-eastern TG sites (latitude $< 30^{\circ}\text{N}$) show similar low-pressure systems carrying
intense PWC and causing strong wind. For northern TGs, such as TGs 1-3 (Supplementary Figs. S1- S3),
the low-pressure systems are less developed compared to other TG sites. As most typhoons make landfall
along the south-eastern China coasts, their intensity decreases when they move from south to north (see
also Fig. 1).

270 **4.5 Impacts caused by compound and non-compound flood events**

To understand impacts caused by compound and non-compound events, we calculated death toll, people
affected, and economic losses for both classes of flooding events. Here we identify compound and non-
compound events in the same way we did for the synoptic weather type analysis. The impact data base
does not include information on all events that we identified, as not all of them led to significant impacts
275 or the impacts were not recorded. A total number of 42 compound flood events (HH) are identified for
Hong Kong, 135 events with high surge and low precipitation (HL), and 160 events for low surge and
high precipitation (LH). As shown in Fig. 8, compound flood events caused 225 deaths, affected 26,718
people, and led to US\$ 221 million in damages. Non-compound flood events caused 63 deaths, affected
4623 people, and caused US\$ 0.16 million recorded damage. Hence, compound flooding events
280 contributed 78% of the reported casualties, 85% of the people affected, and almost recorded damage.

[Fig. 8]

5 Conclusions

In this study, we demonstrate that compound flood events comprised of high surge and heavy precipitation
can occur along major stretches of coastal China. The results show that significant dependence exists
285 between the two flood drivers at many locations, especially at sites in lower latitudes (latitude $< 25^{\circ}\text{N}$).



The dependence varies when using different thresholds in the event sampling and is also affected by seasonality. The latter shows that compound events occur more often during the typhoon season, especially in summer. In terms of weather patterns, compound events at south-eastern TG sites (latitude < 30°N) are caused by low-pressure systems of similar characteristics carrying intense PWC and causing strong winds that generate storm surges. For Hong Kong, we find that compound flooding events were responsible for the vast majority of the recorded casualties and damages, as opposed to flooding events where only one driver was extreme. We also find SLR plays an important role for increasing occurrence of compound events. As SLR keeps rising, it will keep exacerbating the compound effects of flood drivers.

One of the main limitations of this study is the relatively small number of tide gauge sites and limited length of the time-series available, especially from TGs. For now, publicly accessible datasets considered here constitute the most comprehensive collection of hourly sea level data along Chinese coasts. There is an urgent need for longer data sets to be used in order to better assess compound flood risk, especially for south-east China coasts which are prone to TCs. Here we only consider two drivers of flooding, precipitation and storm surge. The role of other flooding drivers needs to be further explored, as well as compound effects under nonstationary conditions, including bivariate frequency analysis, assessing the relationship to climate indices, and the implications for flood risk management. The latter is particularly important, given the low capacity of drainage systems in many Chinese urban areas.

Ignoring compound effects likely leads to an underestimation of flood risk in coastal China, particularly along the south-eastern coasts. It is therefore crucial that coastal cities and urban planning authorities address compound flood effects (including additional drivers such as river discharge or waves) when designing coastal infrastructure and flood defences or developing adaptation plans to combat the negative impacts of climate change.

References

Arns, A., Wahl, T., Haigh, I.D., Jensen, J. and Pattiaratchi, C., 2013. Estimating extreme water level probabilities: a comparison of the direct methods and recommendations for best practise. *Coastal Engineering*, 81, pp.51-66.



- Bevacqua, E., Maraun, D., Vousdoukas, M.I., Voukouvalas, E., Vrac, M., Mentaschi, L. and Widmann, M., 2019. Higher probability of compound flooding from precipitation and storm surge in Europe under anthropogenic climate change. *Science advances*, 5(9), p.eaaw5531.
- Bevacqua, E., Vousdoukas, M.I., Shepherd, T.G. and Vrac, M., 2020. Brief communication: The role of using precipitation or
315 river discharge data when assessing global coastal compound flooding. *Natural Hazards and Earth System Sciences*, 20(6), pp.1765-1782.
- Buchanan, M.K., Oppenheimer, M. and Kopp, R.E., 2017. Amplification of flood frequencies with local sea level rise and emerging flood regimes. *Environmental Research Letters*, 12(6), p.064009.
- Caldwell, P. C., M. A. Merrifield, P. R. Thompson (2015), Sea level measured by tide gauges from global oceans — the Joint
320 Archive for Sea Level holdings (NCEI Accession 0019568), Version 5.5, NOAA National Centers for Environmental Information, Dataset, doi:10.7289/V5V40S7W.
- Chen, W.B. and Liu, W.C., 2014. Modeling flood inundation induced by river flow and storm surges over a river basin. *Water*, 6(10), pp.3182-3199.
- Cheng X. (2020) Flood Risk and Flood Management Policies in China. In: Wang W., Liu Y. (eds) Annual Report on China's
325 Response to Climate Change (2017). Research Series on the Chinese Dream and China's Development Path. Springer, Singapore
- Coles, S., Bawa, J., Trenner, L. and Dorazio, P., 2001. An introduction to statistical modeling of extreme values (Vol. 208). London: Springer.
- Compo, G.P., Whitaker, J.S., Sardeshmukh, P.D., Matsui, N., Allan, R.J., Yin, X., Gleason, B.E., Vose, R.S., Rutledge, G.,
330 Bessemoulin, P. and Brönnimann, S., 2011. The twentieth century reanalysis project. *Quarterly Journal of the Royal Meteorological Society*, 137(654), pp.1-28.
- Couasnon, A., Eilander, D., Muis, S., Veldkamp, T. I. E., Haigh, I. D., Wahl, T., Winsemius, H. C., and Ward, P. J.: Measuring compound flood potential from river discharge and storm surge extremes at the global scale, *Nat. Hazards Earth Syst. Sci.*, 20, 489–504, <https://doi.org/10.5194/nhess-20-489-2020>, 2020.
- 335 Couasnon, A., Eilander, D., Muis, S., Veldkamp, T.I., Haigh, I.D., Wahl, T., Winsemius, H. and Ward, P.J., Measuring compound flood potential from river discharge and storm surge extremes at the global scale and its implications for flood hazard.
- Ding, X.L., Zheng, D.W., Chen, Y.Q. and Huang, C., 2002. Sea level change in Hong Kong from tide gauge records. *Journal of Geospatial Engineering*, 4(1), pp.41-50.
- 340 Du, S., He, C., Huang, Q., & Shi, P. 2018. How did the urban land in floodplains distribute and expand in China from 1992–2015?. *Environmental Research Letters*, 13(3).
- Fang Y, Du S, Scussolini P, et al. Rapid Population Growth in Chinese Floodplains from 1990 to 2015[J]. *International Journal of Environmental Research and Public Health*, 2018, 15(8): 1-11.



- Fang, J., Lincke, D., Brown, S., Nicholls, R.J., Wolff, C., Merkens, J.L., Hinkel, J., Vafeidis, A.T., Shi, P. and Liu, M., 2020.
345 Coastal flood risks in China through the 21st century—An application of DIVA. *Science of the Total Environment*, 704,
p.135311.
- Fang, J., Liu, W., Yang, S., Brown, S., Nicholls, R.J., Hinkel, J., Shi, X. and Shi, P., 2017. Spatial-temporal changes of coastal
and marine disasters risks and impacts in Mainland China. *Ocean & coastal management*, 139, pp.125-140.
- Feng J, von Storch H, Jiang W, et al. (2015). Assessing changes in extreme sea levels along the coast of China. *Journal of*
350 *Geophysical Research: Oceans*, 120(12): 8039-8051.
- Feng X, Tsimplis M N. (2014). Sea level extremes at the coasts of China. *Journal of Geophysical Research: Oceans*, 119(3):
1593-1608.
- Feng, J., Li, D., Wang, T., Liu, Q., Deng, L. and Zhao, L., 2019. Acceleration of the Extreme Sea Level Rise Along the Chinese
Coast. *Earth and Space Science*. <https://doi.org/10.1029/2019EA000653>
- 355 Ganguli, P. and Merz, B., 2019. Trends in compound flooding in northwestern Europe during 1901–2014. *Geophysical*
Research Letters, 46(19), pp.10810-10820.
- Hao, Z., Singh, V.P. and Hao, F., 2018. Compound extremes in hydroclimatology: a review. *Water*, 10(6), p.718.
- He, H., Yang, J., Gong, D., Mao, R., Wang, Y., & Gao, M. (2015). Decadal changes in tropical cyclone activity over the
western North Pacific in the late 1990s. *Climate Dynamics*, 45(11-12), 3317-3329.
- 360 He, H., Yang, J., Wu, L., Gong, D., Wang, B. and Gao, M., 2016. Unusual growth in intense typhoon occurrences over the
Philippine Sea in September after the mid-2000s. *Climate Dynamics*, pp.1-18.
- Hendry, A., Haigh, I., Nicholls, R., Winter, H. and Neal, R., 2019, April. Assessing the characteristics and likelihood of
compound flooding events around the UK. *Hydrol. Earth Syst. Sci.*, 23, 3117–3139.
- Hu, P., Zhang, Q., Shi, P., Chen, B. and Fang, J., 2018. Flood-induced mortality across the globe: Spatiotemporal pattern and
365 influencing factors. *Science of The Total Environment*, 643, pp.171-182.
- Jiang T., Su B., Huang J. et al. Each 0.5°C of warming increases annual flood losses in China by more than 60 billion USD.
Bull. Amer. Meteor. Soc. (2020). <https://doi.org/10.1175/BAMS-D-19-0182.1>.
- Khanal, S., Ridder, N., Terink, W. and Hurk, B.V.D., 2019. Storm surge and extreme river discharge: a compound event
analysis using ensemble impact modelling. *Frontiers in Earth Science*, 7, p.224.
- 370 Kojadinovic, I. and Yan, J., 2010. Modeling multivariate distributions with continuous margins using the copula R package.
Journal of Statistical Software, 34(9), pp.1-20.
- Kundzewicz, Z.W., Su, B., Wang, Y., Xia, J., Huang, J. and Jiang, T., 2019. Flood risk and its reduction in China. *Advances*
in Water Resources, 130, pp.37-45.
- Lai Y., Li J., Gu Xi., et al. Greater flood risks in response to slowdown of tropical cyclones over the coast of China. *Proceedings*
375 *of the National Academy of Sciences*, 2020; 117 (26): 14751 DOI: 10.1073/pnas.1918987117.



- Leonard, M., Westra, S., Phatak, A., Lambert, M., van den Hurk, B., McInnes, K., Risbey, J., Schuster, S., Jakob, D. and Stafford-Smith, M., 2014. A compound event framework for understanding extreme impacts. *Wiley Interdisciplinary Reviews: Climate Change*, 5(1), pp.113-128.
- Lian, J. J., Xu, K., and Ma, C.: Joint impact of rainfall and tidal level on flood risk in a coastal city with a complex river network: a case study of Fuzhou City, China, *Hydrol. Earth Syst. Sci.*, 17,679–689, <https://doi.org/10.5194/hess-17-679-2013>, 2013.
- Liu J, Wen J, Huang Y, et al. Human settlement and regional development in the context of climate change: a spatial analysis of low elevation coastal zones in China[J]. *Mitigation and Adaptation Strategies for Global Change*, 2015, 20(4): 527-546.
- Marcos, M., Rohmer, J., Vousdoukas, M.I., et al., 2019. Increased Extreme Coastal Water Levels Due to the Combined Action of Storm Surges and Wind Waves. *Geophysical Research Letters*, 46(8), pp.4356-4364.
- Moftakhari, H. R., Salvadori, G., AghaKouchak, A., Sanders, B. F., & Matthew, R. A. (2017). Compounding effects of sea level rise and fluvial flooding. *Proceedings of the National Academy of Sciences*, 114(37), 9785-9790.
- Paprotny, D., Vousdoukas, M.I., Morales-Nápoles, O., Jonkman, S.N. and Feyen, L., 2018. Compound flood potential in Europe. *Hydrol. Earth Syst. Sci. Discuss*, 2018, pp.1-34.
- Petroliaqkis, T.I., Voukouvalas, E., Disperati, J. and Bidlot, J., 2016. Joint probabilities of storm surge, significant wave height and river discharge components of coastal flooding events. *European Commission-JRC Technical Reports*.
- Qin H, Li Z, Fu G, et al. The effects of low impact development on urban flooding under different rainfall characteristics[J]. *Journal of Environmental Management*, 2013: 577-585.
- Svensson, C. and Jones, D.A., 2002. Dependence between extreme sea surge, river flow and precipitation in eastern Britain. *International Journal of Climatology: A Journal of the Royal Meteorological Society*, 22(10), pp.1149-1168.
- Svensson, C. and Jones, D.A., 2004. Dependence between sea surge, river flow and precipitation in south and west Britain. *Hydrology and Earth System Sciences*, 8(5), pp.973-992.
- Urban Planning & Design Institute of Shenzhen, China, 2008. Detailed Planning for Reclaimed Water and Stormwater Utilization in Guang-ming New District in Shenzhen. (in Chinese).
- van den Hurk, B., van Meijgaard, E., de Valk, P., van Heeringen, K.J. and Gooijer, J., 2015. Analysis of a compounding surge and precipitation event in the Netherlands. *Environmental Research Letters*, 10(3), p.035001.
- Wahl, T., Jain, S., Bender, J., Meyers, S.D. and Luther, M.E., 2015. Increasing risk of compound flooding from storm surge and rainfall for major US cities. *Nature Climate Change*, 5(12), p.1093.
- Ward, P.J., Couasnon, A., Eilander, D., Haigh, I.D., Hendry, A., Muis, S., Veldkamp, T.I., Winsemius, H.C. and Wahl, T., 2018. Dependence between high sea-level and high river discharge increases flood hazard in global deltas and estuaries. *Environmental Research Letters*, 13(8), p.084012.
- Wu S., et al. Shortening the recurrence periods of extreme water levels under future sea-level rise. *Stochastic Environmental Research and Risk Assessment*, 2017, 31(10):2573-2584.



- 410 Wu, L., Wang, B., & Geng, S. (2005). Growing typhoon influence on east Asia. *Geophysical Research Letters*, 32(18), 109-127.
- Wu, W., McInnes, K., O'grady, J., Hoeke, R., Leonard, M. and Westra, S., 2018. Mapping dependence between extreme rainfall and storm surge. *Journal of Geophysical Research: Oceans*, 123(4), pp.2461-2474.
- Xing, Z., Yan, D., Zhang, C., Wang, G. and Zhang, D., 2015. Spatial Characterization and Bivariate Frequency Analysis of Precipitation and Runoff in the Upper Huai River Basin, China. *Water Resources Management*, 29(9), pp.3291-3304.
- 415 Xu, H., Xu, K., Lian, J., & Ma, C. (2019). Compound effects of rainfall and storm tides on coastal flooding risk. *Stochastic Environmental Research and Risk Assessment*, 1-13.
- Xu, K., Ma, C., Lian, J. and Bin, L., 2014. Joint probability analysis of extreme precipitation and storm tide in a coastal city under changing environment. *PloS one*, 9(10), p.e109341.
- Yap, W., Lee, Y., Gouramanis, C., Switzer, A.D., Yu, F., Lau, A.Y.A. and Terry, J.P., 2015. A historical typhoon database for the southern and eastern Chinese coastal regions, 1951 to 2012. *Ocean & Coastal Management*, 108, pp.109-115.
- 420 Ye, Y. and Fang, W., 2018. Estimation of the compound hazard severity of tropical cyclones over coastal China during 1949–2011 with copula function. *Natural Hazards*, 93(2), pp.887-903.
- Zhai, P., Zhang, X., Wan, H. and Pan, X., 2005. Trends in total precipitation and frequency of daily precipitation extremes over China. *Journal of climate*, 18(7), pp.1096-1108.
- 425 Zheng, F., Westra, S., Leonard, M. and Sisson, S.A., 2014. Modeling dependence between extreme rainfall and storm surge to estimate coastal flooding risk. *Water Resources Research*, 50(3), pp.2050-2071.
- Zscheischler, J., Westra, S., Van Den Hurk, B.J., Seneviratne, S.I., Ward, P.J., Pitman, A., AghaKouchak, A., Bresch, D.N., Leonard, M., Wahl, T. and Zhang, X., 2018. Future climate risk from compound events. *Nature Climate Change*, 8(6), pp.469-477.

430

Acknowledgements. This work is funded by the National Key R & D Program of China (2017YFC1503001; 2017YFE0100700); Shanghai Sailing Program (19YF1413700); China Postdoctoral Science Foundation (No. 2019M651429). TW acknowledges funding support from the National Science Foundation (Grant Number 1929382).

435

Author contributions. FJ (first author) and TW conceived and planned the study. FJ (first author) carried out the analysis and prepared the paper. TW provided guidance on compound flood analysis and contributed to interpretations. FJ (third author), KF, SX and LM offered their expertise in flood, heavy precipitation and hydrometrology, and contributed to revising the manuscript.

440

Competing interests. The authors declare that they have no conflict of interest.



Data availability. This study relies entirely on publicly available data from 1) hourly sea-level data of 11 TGs with at least 20-year lengths along the Chinese coast from the University of Hawaii Sea Level Center; 2) cumulative daily precipitation records from 1951-2015 are collected from China Meteorological Administration.;3) meteorological data from the 20th Century Reanalysis, Version 2c, obtained from the National Oceanic and Atmospheric Administration website; 4) historical damages records from a typhoon database developed by Yap et al. (2015) including historical typhoon records from 1951 to 2012.

Supplementary. Meteorological patterns for associated with compound and non-compound events at the other 9 TGs (not shown in the manuscript) are shown in the supplementary.

455

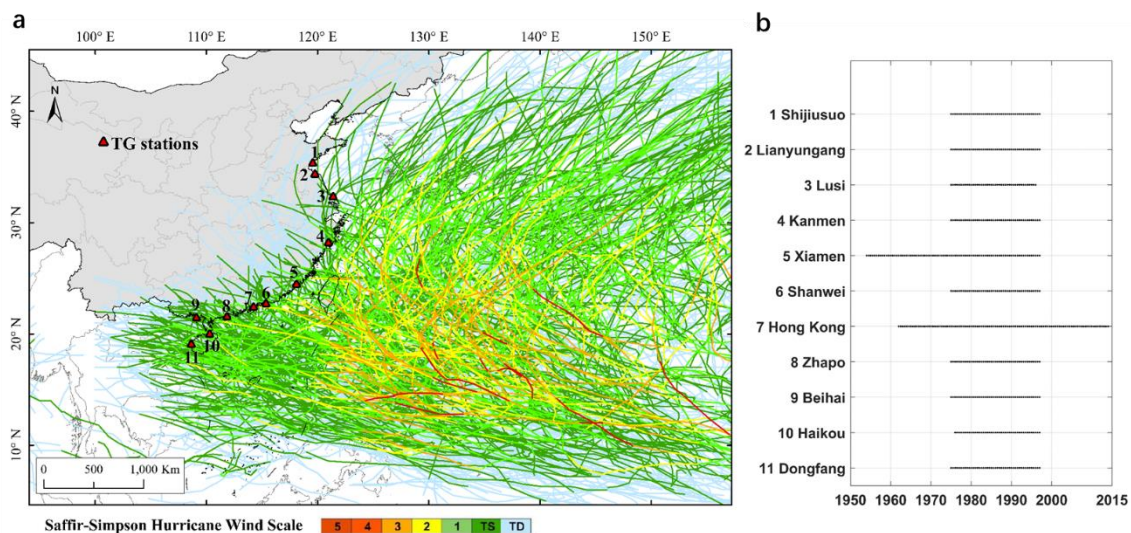


Fig.1 (a) Locations of 11 tide gauges and historical typhoon tracks for different intensities (only 1975-1997 shown here); (b) time periods covered by hourly data at the 11 tide gauges.

460

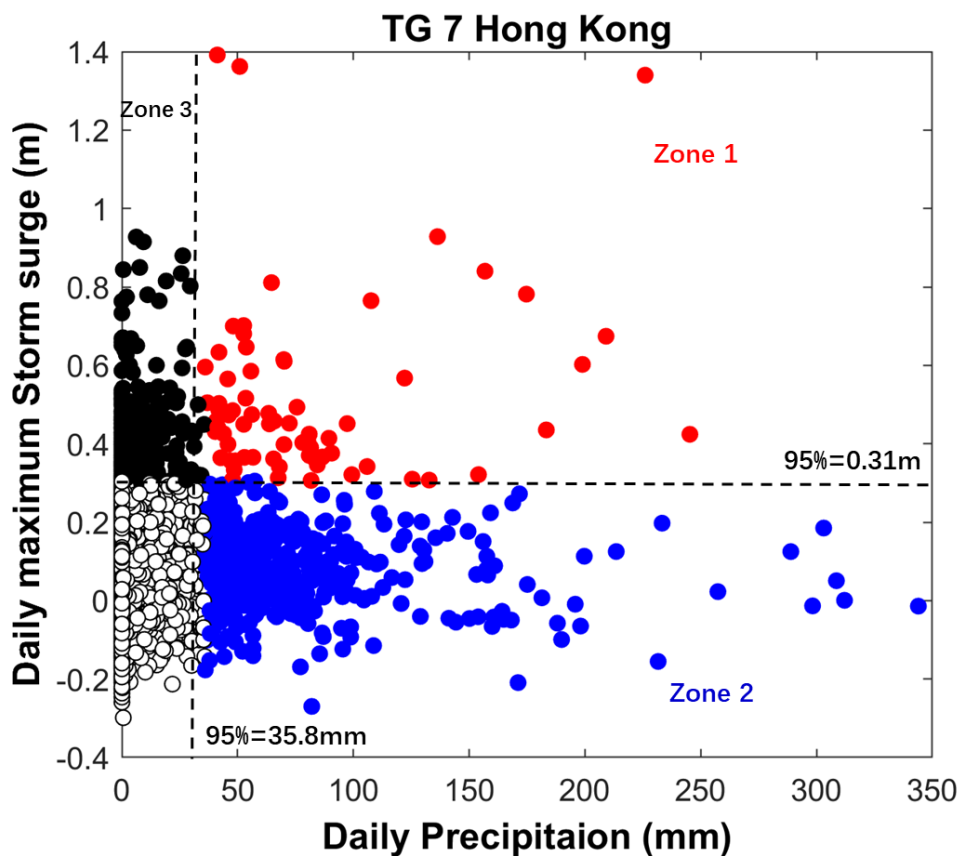
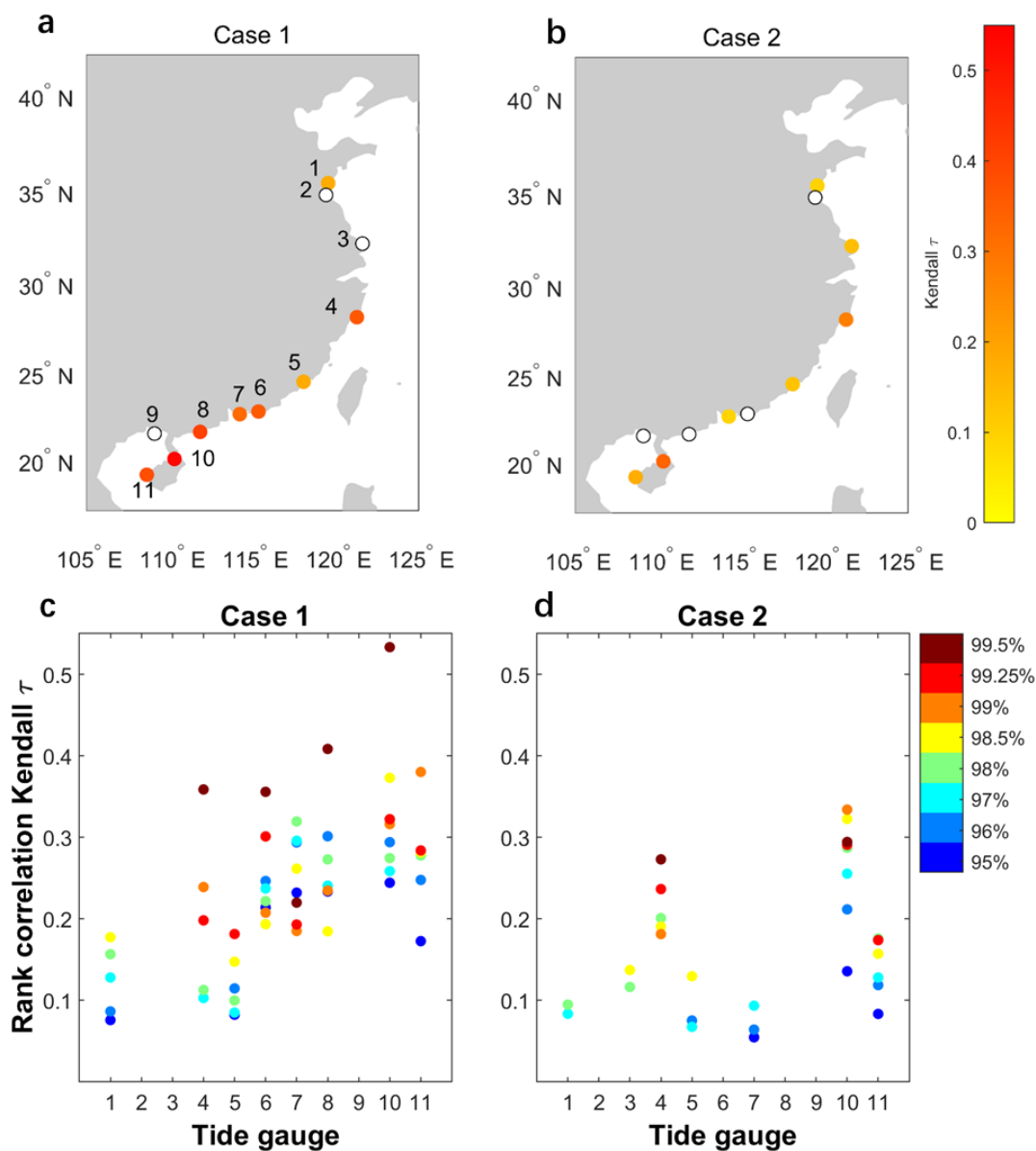
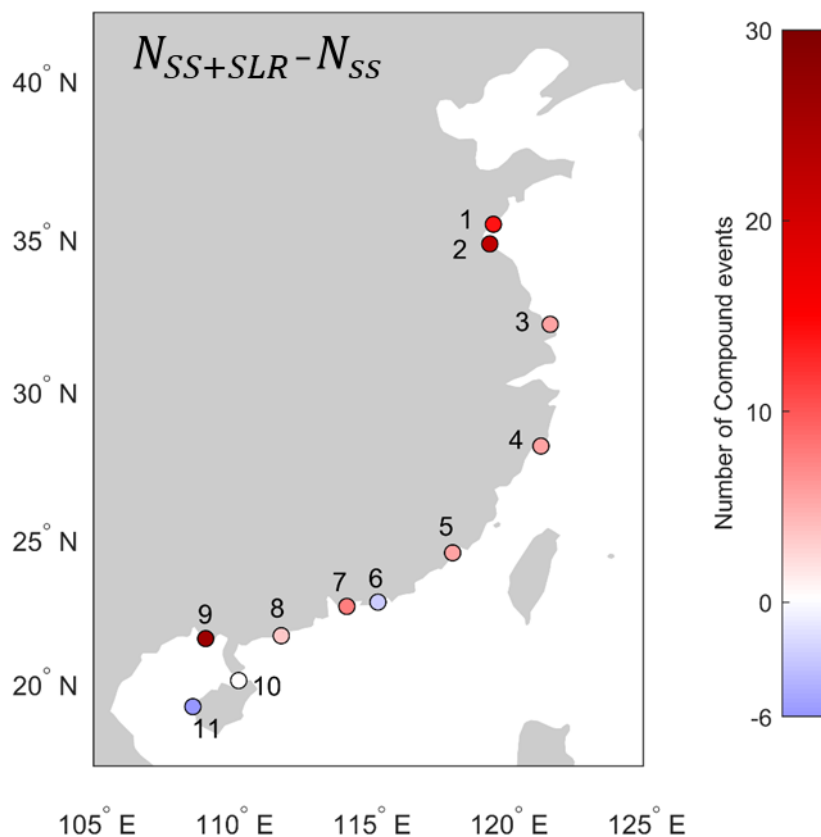


Fig. 2 Daily maximum storm surge plotted against daily maximum precipitation for threshold of 98%. Case 1 indicates Zone1
465 and Zone3. Case 2 indicates zone1 and zone2. Red dots (plotted in Zone 1) show the events with potential for compound
flooding (i.e. joint occurrence of high storm surge and heavy precipitation), whereas blue (Zone 2) and black (Zone 3) dots
define the non-compound events (i.e. high storm surge or high precipitation only, respectively).

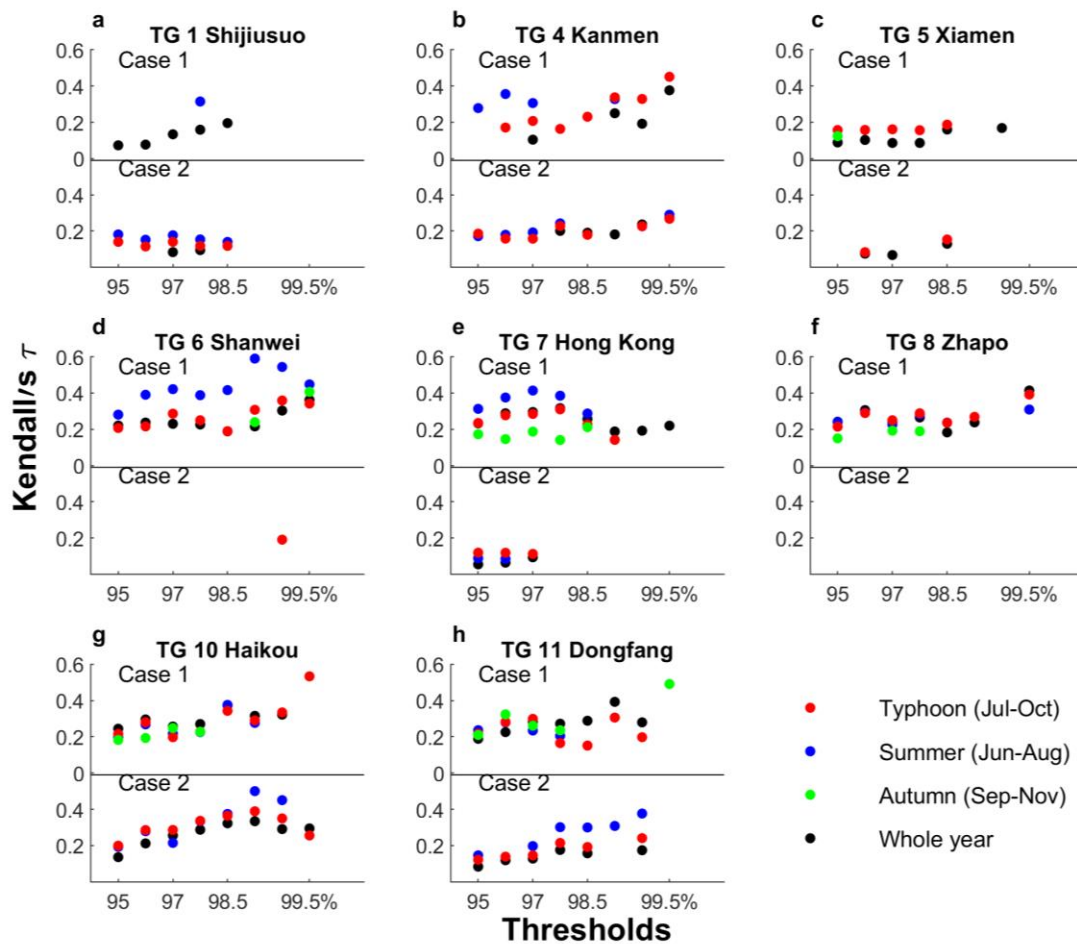


470 Fig. 3 Kendall's tau between storm surge and precipitation for thresholds from 95% to 99.5% for Case 1 (a and c) and Case 2 (b and d). Maximum dependence was plotted for Case 1 and Case2 in a) and b), white dots refer to insignificant dependence (10% level). Only significant results at the 90% confidence level are shown in c) and d).

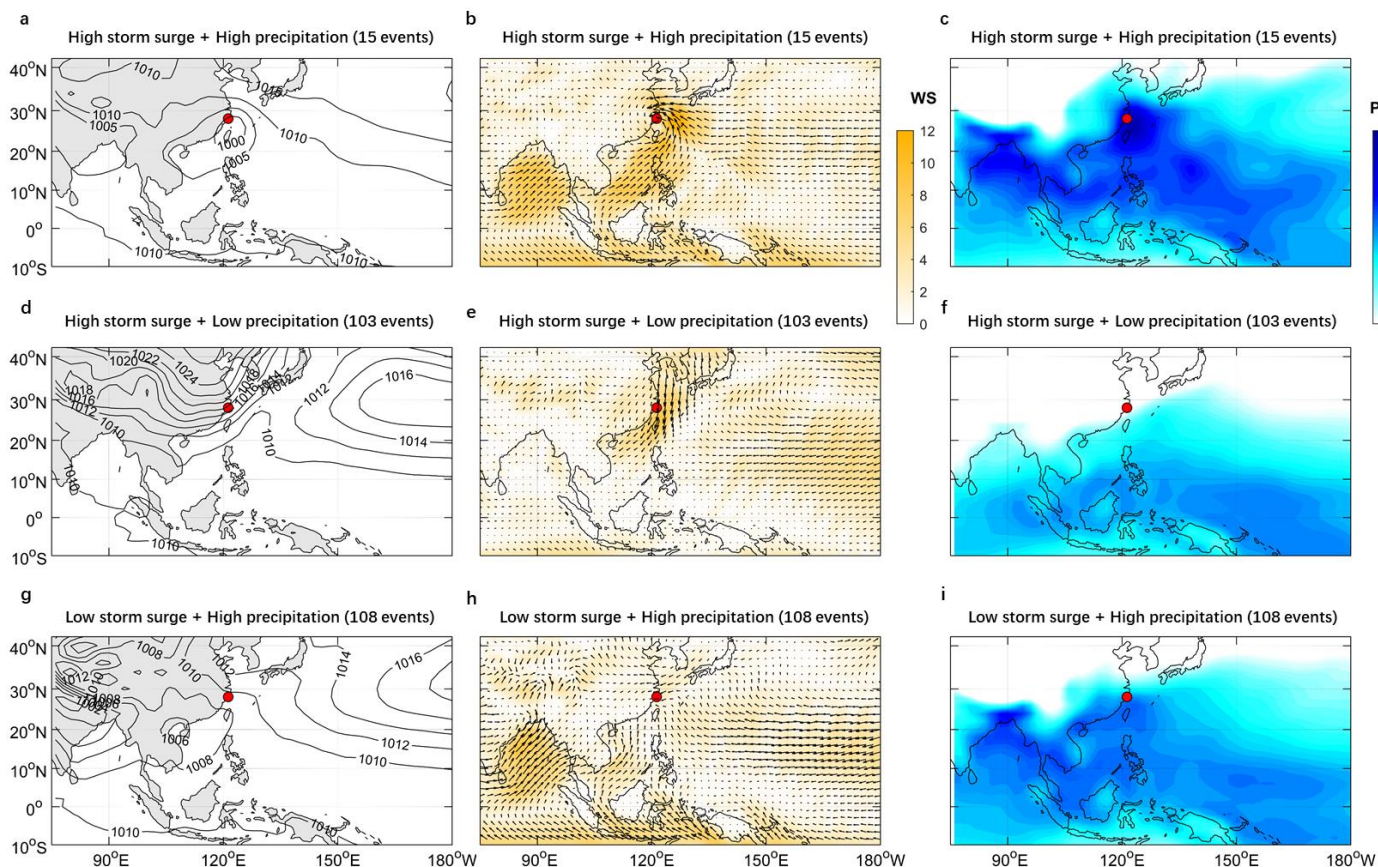


475

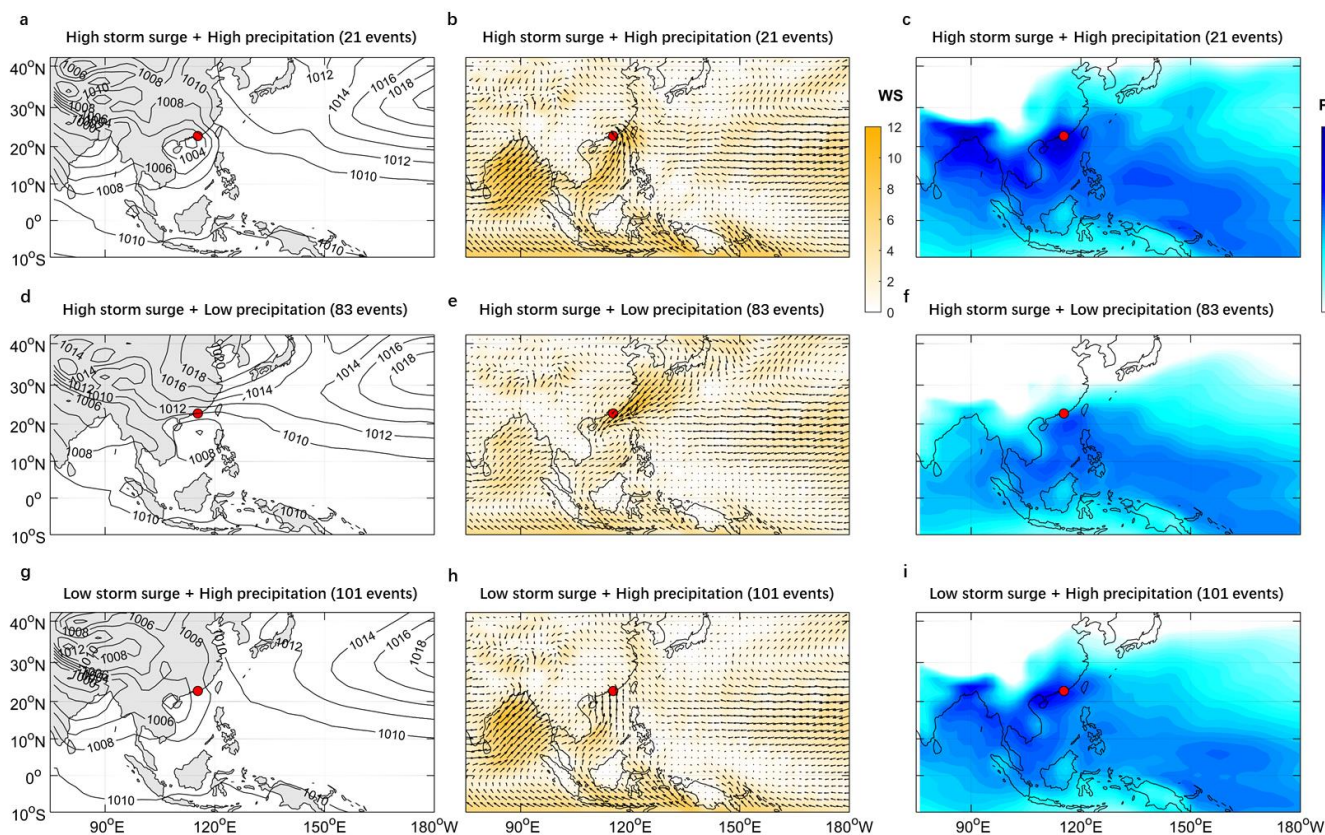
Fig. 4 Counts of compound events between storm surge and precipitation with/without sea level rise at threshold of 98% (falling in Zone 1 in Fig. 2). N_{SS+SLR} indicates compound events between storm surge considering historical sea level rise trend. N_{SS} indicates compound events between storm surge by removing annual mean sea level.



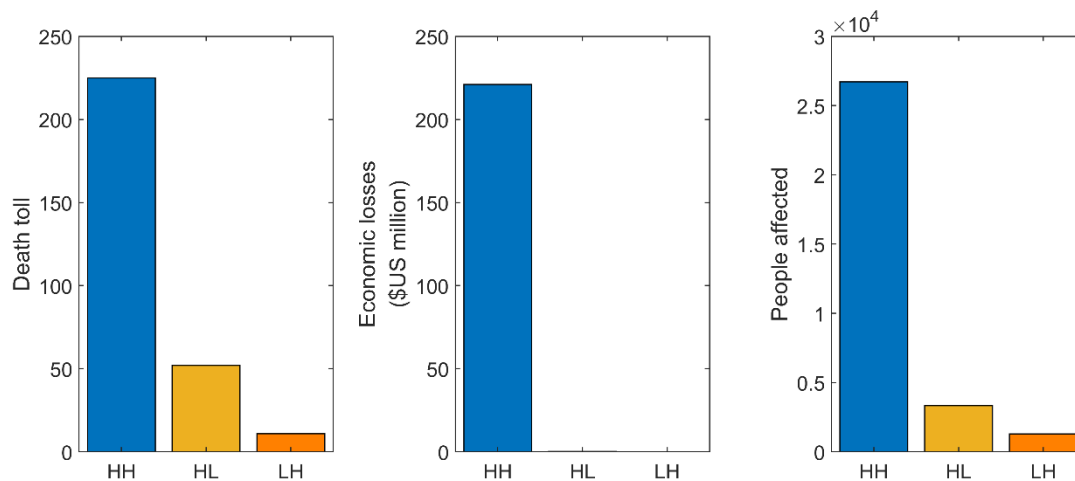
480 Fig. 5 Kendall's tau between storm surge and precipitation in summer, autumn, the typhoon season, and the whole year for different thresholds used in the POT sampling for Case 1 (a) and Case 2 (b) (Only significant dependences at the 90% confidence level are shown).



485 Fig. 6 Meteorology conditions for Kanmen (TG 4): (a, d, g) sea-level pressure (mbar), (b, e, h) wind speed (m/s) and direction (grey arrows), and (c, f, i) precipitable water content (PWC, kg m^{-2}) during (a, b, c) compound events with high storm surge and high precipitation, (d, e, f) for non-compound events with high storm surge and low precipitation, and (g, h, i) non-compound events with low storm surge and high precipitation.



490 Fig. 7 Meteorology conditions for Shanwei (TG 6): (a, d, g) sea-level pressure (mbar), (b, e, h) wind speed (m/s) and direction (grey arrows), and (c, f, i) precipitable water content (kg m⁻²) during (a, b, c) compound events with high storm surge and high precipitation, (d, e, f) for non-compound events with high storm surge and low precipitation, and (g, h, i) non-compound events with low storm surge and high precipitation.



495 Fig. 8 Damages by compound (HH: high storm surge and high precipitation) flood and non-compound flood events (HL refers to high storm surge and low precipitation; LH refers to low storm surge and high precipitation) in Hong Kong.